Adsorption applications of unmodified geothermal silica

Article *in* Geothermics · April 2014

DOI: 10.1016/j.geothermics.2013.08.001

CITATIONS
6

READS
241

3 authors, including:

Halldor Gudfinnur Svavarsson
Reykjavik University
62 PUBLICATIONS **462** CITATIONS
SEE PROFILE

Sigurbjorn Einarsson
KeyNatura ehf.
6 PUBLICATIONS **83** CITATIONS
SEE PROFILE

Adsorption applications of unmodified geothermal silica

Halldor G. Svavarsson[a,b,*], Sigurbjorn Einarsson[a], Asa Brynjolfsdottir[a]

[a] Blue Lagoon Ltd. Iceland

[b] School of Science and Engineering, Reykjavík University, Iceland

[*] Corresponding author at: School of Science and Engineering, Reykjavík University, Iceland. Tel.: +354 5996200; fax: +354 5996201. *E-mail address*: halldorsv@ru.is (H.G. Svavarsson).

ABSTRACT

Silica, precipitated out of geothermal fluid discharged from a geothermal powerplant in Svartsengi on the Reykjanes peninsula in Iceland, was used as a chromatographic adsorbent to extract blue colored protein, C-Phycocyanin, from *coccoid* blue-green algae. The only supplement used was salt obtained by evaporating the geothermal fluid. Analysis of the silica, using scanning electron microscopy, X-ray diffractometry and Brunauer-Emmett-Teller (BET) adsorption confirmed it has a high specific surface area and is amorphous. Upon adsorption and subsequent elution the purity of the extracted protein, measured as the ratio of the light absorbance of 620 and 280 nm, increased from 0.5 to above 2.0. Our results could facilitate utilization of a mostly unused byproduct of geothermal powerplants as chromatographic material.

Keywords:

Geothermal silica

Chromatographic

Adsorption

Protein separation

Phycocyanin

1. Introduction

1.1 Geothermal Silica

Geothermal resources are widespread throughout the world although generally associated with areas of volcanic activity. The HS-Energy geothermal powerplant is located in Svartsengi on the Reykjanes peninsula, south-west Iceland on a sequence of lava flows, the youngest being roughly 800 years old (Saemundsson et al., 2010). The geological structure is further characterised by interlayers of scoria and hyaloclastite reflecting interglacial and glacial periods. Since the lava flows, scoria and interlayers of hyaloclastite are highly porous and permeable, they allow seawater to percolate deep into their aquifers where it heats up and mixes with meteoric water (Arnorsson, 1995). Geothermal wells drilled through the lava flows to depths of up to 2,000 m discharge a mixture (here referred to as geothermal fluid) of 2/3 seawater and 1/3 meteoric water with a temperature of about 240°C. Due to leaching, the hot geothermal fluid contains a high concentration of silicon (Si) when it enters the wells. Originally, the silicon is present in the hot geothermal fluid as silicic acid $(SiO_x(OH)_{4-2x})_n$. Upon cooling, the silicic acid precipitates as a three-dimensional network of coagulated primary silica (SiO_2) particles. The primary particles grow up to some nanometers in size before they coagulate to form aggregated clusters. Such a small particle size gives rise to high specific surface area, which makes the SiO_2 a suitable candidate for adsorption and catalytic applications.

Steam from the flashed geothermal fluid is used to produce electricity (output power of ~75 MW_e). The residual liquid is used in a heat exchange process (output power of ~150 MW_t) to heat up freshwater for district heating of local communities of roughly 20,000 habitants. This heat exchange process limits the minimum temperature for heat extraction of the geothermal fluid to about 90°C. Most of the spent geothermal fluid is reinjected into the geothermal reservoir (~6×10^6 m^3 annually) but some of it (~1.2×10^6 m^3 annually) is discharged on the surface where it forms the Blue Lagoon (Grether-Beck et al., 2008; Petursdottir et al., 2009). A small fraction of the discharged fluid is bypassed to sedimentation tanks at the Blue Lagoon where it cools from 90°C to ambient temperature. The cooling causes supersaturation of the silicic acid which in turn precipitates as amorphous SiO_2. The pH of the resulting supernatant

is 7.7 ±0.2, sligthly higher than the pH of the Blue Lagoon which is 7.5 ±0.2. At 90°C, the geothermal fluid contains about 600 ppm SiO_2 and thus the 7×10^6 m^3 of liquid being discharged and reinjected annually carries about 4,000 tonnes. At 10-15°C, a realistic ambient temperature, the SiO_2 concentration has dropped by roughly an order of magnitude (Fleming and Crerar, 1982) and thus a precipitation of over 3,000 tonnes could potentially be harnessed annually from fluid discharged from the HS-Energy facility alone.

Few authors have reported on practical applications of modified geothermal SiO_2 and still fewer on applications of unmodified SiO_2. A possible use of geothermal SiO_2 as a filler in paper (Johnston et al., 2004) and as a precursor for silicates (Gallup et al., 2003) has been described. In both cases the precipitation conditions had to be controlled. The use of natural SiO_2, modified with organosilicate materials, as a chromatographic material has also been discussed (Tarasevich et al., 1990).

1.2 Chromatographic silica

Silica gel ($SiO_2 \cdot xH_2O$) is widely used as an adsorbent in chromatographic columns for isolation and purification of compounds from a mixture. One of the most common methods for the analysis of basic pharmaceuticals is liquid chromatography (McKeown et al., 2001), which conventionally relies on synthetic silica and silica derivatives as the stationary phase. The production of synthetic chromatographic silica typically involves several chemical reaction steps followed by a series of after-treatment processes (Hoffmann et al., 2006; Zhang et al., 2009). In this paper we discuss the chromatographic application of unmodified geothermal silica. A comparison to sintered geothermal silica is also made.

1.3 Phycocyanin

The Blue Lagoon is a specific geothermal biotope known for its unique microbial ecosystem (Petursdottir and Kristjansson, 1997; Petursdottir et al., 2009). It contains about 6,000 m^3 of geothermal fluid that is replenished every 40 h. The lagoon′s temperature remain constant at 38 ±1°C. The coccoid blue-green algae, *Cyanobacterium aponinum*, one of the dominating species in the microbial ecosystem, is used in this research. A water-soluble photosynthetic pigment in blue-green algae, Phycocyanin (C-PC), is a protein that belongs to a family of phycobiliproteins. It is an accessory pigment to the green-colored pigment chlorophyll, also found in blue-green algae. Together they are an essential component of the algae′s light harvesting system (McCall, 1998). Phycobiliproteins have in common a similar three-dimensional structure in addition to their hydrophilic nature. Among the many interesting

applications of C-PC is its use as a fluorescent marker of cells and macromolecules (Ramos et al., 2010) and as a natural colorant in food and cosmetic products, replacing synthetic dyes, which are often unsafe or even toxic. C-PC has also been shown to exhibit bio-activity (Eriksen, 2008) which makes it an excellent choice as an additive in food and pharmaceutical products. However, the use of C-PC in these products is dependent on obtaining the appropriate grade of purity. The purity of C-PC can be evaluated as the ratio between the light absorbance at λ = 620 nm and 280 nm (A_{620}/A_{280}), where A_{620nm} is the maximum absorbance of C-PC and A_{280nm} is the total absorbance of proteins. A purity of 0.7 is considered food grade, 3.9 reactive grade and greater than 4.0 analytical grade (Rito-Palomares et al., 2001). Despite the many possible applications of phycobiliproteins, their use is limited by the high cost of extraction and purification. Most of the methods used for purification of C-PC involve a sequence of operations that include precipitation, centrifugation, dialysis, ion-exchange and gel filtration chromatography and chromatography on hydroxyapatite (Rito-Palomares et al., 2001). The purification cost has been estimated at 50-90% of the total production cost (Patil et al., 2006). Thus, improvements in the purification procedure can lead to a significant reduction in the production cost. C-PC is unstable to heat and light in an aqueous solution and denatures at temperatures above 45°C (Jespersen et al., 2005). This instability puts constraints on the possible processing methods that can be used. In the experiments described in this paper, unmodified geothermal SiO_2 precipitated from Blue Lagoon geothermal fluid was used as an alternative to other chromatographic materials to extract C-PC from the coccoid blue-green alga, *cyanobacterium aponinum*. When SiO_2 powder was soaked in a saline solution of a ruptured cell mass, the C-PC was selectively adsorbed in contrast to other hydrophobic constituents (such as chlorophyll). The attached C-PC was released from the SiO_2 adsorbent by washing with deionized water.

2. Experimental Conditions

2.1 Algae cultivation

Blue-green algae, isolated from the Blue Lagoon, were cultivated in a semi-continuous mode in a 1.2 m^3 tubular photobioreactor at 45°C at the Blue Lagoon Research and Development Center in Iceland. The cultivation media was geothermal fluid with 0.3% mass/vol Cell-hi WP nutrient. Illumination was provided by a high pressure sodium light (160 µE/m^2/s). A fixed pH of 7.5 was maintained by regulating the CO_2 gas feed rate during growth. At harvesting,

the algae suspension contained 12.2% wt. dry weight of algae. A 360 ml volume of the suspension was homogenized for 10 min using a 900 W ultrasonic cell crusher at 20 kHz (SYJ900-D from Sharpertek) with a duty cycle of 2 s on and 3 s off. Subsequently, the solution was centrifuged at 3200 × g for 10 min. A 288 ml volume of supernatant (referred to as crude extract) was obtained and collected.

2.2 Chromatographic silica

Raw materials used for the chromatographic recovery of C-PC consisted of geothermal SiO_2 (referred to as BL-silica) and geothermal salt (referred to as BL-salt). The chemical composition of the BL-silica and the BL-salt was determined by inductively coupled plasma mass spectrometry (ICP-MS). The BL-silica was removed from the sedimentation tank and pumped into a filtration press at a pressure of 2 bar. The resulting filter cake was dried at 60°C, crushed manually and sieved. After removal of the BL-silica, the BL-salt was prepared by drying the supernatant. The characteristics of the BL-silica (ground in a mortar), before and after sintering at 1000°C for 2 h, was determined using a scanning electron microscope (SEM) and by measuring the specific surface area (BET), t-plot area and Barrett-Joyner-Halenda (BJH) average adsorption pore width (Micromeritics TriStar 3000 Surface Area and Porosity Analyzer). The mineralogy of the BL-silica was determined by X-ray diffraction analysis (XRD: Bruker AXS).

2.3 Protein extraction

Two different approaches for adsorption and subsequent elution were applied; Method 1 and Method 2. In the following discussion, we focus primarily on the latter procedure.

2.3.1 Method 1

BL-silica agglomerates, ranging in size from 0.2 to 0.7 mm, were packed in a 30 cm tall plexiglas column with a diameter of 5 cm. The column was loaded with ~190 ml crude extract (see *2.1 Algae cultivation* above) at a pressure of 0.4 bar. Afterwards, 2.2 l of BL-salt solution (25% wt. BL-salt in deionized water) was pumped through the column to flush the chlorophyll. Subsequently the C-PC was eluted using a continuous flow of 2.0 l deionized water. The pressure was gradually increased from 0.4 to 0.6 bar during pumping of the BL-salt solution and the eluent.

2.3.2 Method 2

BL-silica that passed through a 125 µm mesh screen was mixed with the crude extract and a BL-salt solution. The C-PC discharge was accomplished batchwise by alternating cycles of centrifugation and the addition of deionized water. A 100 ml crude extract (see *2.1 Algae cultivation* above) was mixed with 10 ml of saturated BL-salt solution (approximately 0.36 g salt per ml) and 20 g of BL-silica and then centrifuged. The supernatant was discarded and the sediment was slurried in 50 ml of saline solution (40 ml of deionized water and 10 ml of saturated BL-salt solution) and centrifuged again. This step of slurrying the sediment and centrifuging was repeated with deionized water in discrete volumes of 10 ml. The supernatant, containing eluted C-PC, was collected after each step. A flow sheet of the extraction and the purification process is shown in **Fig. 1**. Absorption values and absorbance spectra of the supernatant (eluent) and the crude extract were measured using a UV-visible Camspec M350 spectrophotometer. The Purity Ratio (PR) of the C-PC was taken as the A_{620nm}/A_{280nm} ratio.

Methods 1 and 2 were repeated with sintered (1000°C/2h) BL-silica, instead of unsintered silica, upon which the binding capacity of the silica was completely lost.

3. Results and discussion

3.1 Protein extraction - Method 1

The proceeding of the column′s loading and elution is visualized in chronological order in **Fig. 2**. As seen, the green colored chlorophyll flows through the column while the C-PC is retained at the stationary BL-silica. A good separation of C-PC was obtained, with a net 3-fold increment in the PR. The column, however, degraded due to compression of the agglomerates during pumping of the eluent. Consequently the flow rate through the column gradually decreased to ~4 ml/min which is impractically low. The possibility of using the geothermal SiO_2 as a stationary phase in the chromatographic column requires further evaluation. An attempt to strengthen the SiO_2 agglomerates with sintering resulted in a total loss of performance accompanied by a decrease of its specific surface area from 60 to 1 m^2 (see **Table 1.**). This problem might be overcome by embedding the unsintered SiO_2 agglomerates in a rigid matrix, but such speculations are beyond the scope of this paper.

3.2 Protein extraction - Method 2

The concentration of C-PC was determined using Eq. (1) (Mishra et al., 2008), where A_{620} and A_{652} are the absorption values at 620 and 652 nm, respectively.

$$C_{\text{C-PC}} = (A_{620}\text{-}0.474A_{652})/(5.34) \text{ [mg/ml]} \qquad (1)$$

A graphical interpretation of the result is given in **Fig. 3**. It is apparent from the figure that the shapes of the concentration and purity curves resemble each other. Both lines rise roughly linearly with increasing eluent volume up to ~140 ml. At higher volumes the concentration decreases throughout the elution while the purity line flattens out rather abruptly at volumes above ~200 ml. The maxima of the PR, ~2.0, and the $C_{\text{C-PC}}$, 6.3 mg/ml, appear at the same eluent volume (~140 ml). As always, there is a trade-off between the purity of the protein and its recovery rate. Several different batches were collected. The 10 ml volume with the highest purity will be referred to as collection #1. The volume fractions with PR $\geq$ 1.0 were later combined, making a total volume of 117 ml (collection #2) with 4.9 mg/ml C-PC and a PR of 1.3, which corresponds to 31% recovery of the C-PC. Combining the volume fractions between 40 and 250 ml resulted in a PR of 1.0 and 50% recovery (collection #3). Absorption spectra, in the range of 250-700 nm, of collections #1 and #2, are shown in **Fig. 4**. A spectrum of the crude extract is shown for comparison.

The PR and $C_{\text{C-PC}}$ values for the crude extract are 0.46 and 18.2 mg/ml, respectively. It therefore contained ~1,800 mg C-PC (100 ml×18.2 mg/ml) whereas the area under the measured concentration curve (Fig. 3.) corresponds to ~1,100 mg. This equals to a total recovery of 61% ((1.1/1.8)×100%). A higher BL-silica/crude-extract ratio might increase the recovery rate of the C-PC but most likely at the expense of its purity.

3.3 Morphology analyses of the chromatographic silica

Values of the specific surface area, micropore surface area, pore volume and average adsorption pore width of the BL-silica, before and after sintering are given in Table 1. **Table 2.** shows the chemical composition of the BL-silica and the BL-salt.

The XRD patterns of sintered and unsintered BL-silica are shown in **Fig. 5**. The amorphous structure of the latter is clearly demonstrated by the absence of sharp diffraction peaks. The dry SiO_2 powder contains ~7% wt. of salt (mainly NaCl). Sharp peaks in Fig. 5 at 2Θ = 31.75° and 45.48° are due to crystalline NaCl present in the BL-silica. After sintering, a strong and sharp peak has appeared at 2Θ = 22°, indicating some of the amorphous SiO_2 has been converted to a crystalline form of SiO_2 (cristobalite). The concentration of NaCl, however, appears to have decreased, as indicated by the lower intensity of the diffraction peaks.

Fig. 6. shows the SEM images at two different magnifications of BL-silica agglomerates before and after sintering. Prior to sintering we see a porous surface composed of particles with diameters ranging from 20 nm to 90 nm. According to Icopini et al. (2005), who investigated oligomerization of SiO_2 as a function of its concentration, ionic strength and pH in natural brine solutions, coagulation occurs when the SiO_2 particles reach ~3 nm in size. Our values of 20-90 nm are much larger than the value they give. However, it must be taken into account that in our case the silica precipitation was triggered by change in temperature from whereas in their case, it was triggered by a change in the pH. Upon sintering the particles have grown and apparently fused together. The porous appearance is no longer visible; instead a glass-like surface has formed. These structural changes may, in part, be attributed to the salt present in the BL-silica. As the sintering temperature of 1000°C is well above the melting point of NaCl (801°C), the SiO_2 could have been coated with the molten salt which solidifies upon cooling. Additional phases, formed by reactions of the SiO_2 and the molten salt, may also be present in a small amount. Crystalline particles, roughly 10 μm on a side, were observed after sintering (see inset in Fig. 6(b).). A further confirmation of the morphological changes occurring in the sintered SiO_2 is indicated by the decrease in the pore volume, from 0.24 to 0.001 cm^3/g (Table 1.). This is consistent with the observed loss of performance of the SiO_2 after sintering. The average pore width of 23 nm is several times the size of the C-PC protein molecule (Fisher et al., 1980). These facts could explain the selective adsorption of C-PC from the crude extract containing chlorophyll and C-PC. It can therefore be speculated that the chromatographic mechanism is size dependent (Paul-Dauphin et al., 2007).

4. Conclusions

A possible use of geothermal SiO_2 as a chromatographic material has been described. SiO_2 deposits have been considered an undesirable byproduct of geothermal power production and large quantities of it can be extracted from geothermal fluid. Its ability to adsorb protein molecules was demonstrated by the separation of C-PC from disrupted blue-green algae mass. A critical factor controlling the adsorption capability is the high specific surface area as observed by loss of performance upon sintering. The process described here has considerable potential as a simple, ecological and inexpensive first step in the purification and separation of natural proteins by utilizing geothermal resources.

Acknowledgements

This research was supported in part by the Icelandic Technology Development Fund and the Energy Fund of the National Energy Authority.

References

Arnorsson S., 1995. Geothermal systems in Iceland: Structure and conceptual models. 1. High-temperature areas, Geothermics 24, 561-602.

Eriksen N.T., 2008. Production of phycocyanin - a pigment with applications in biology, Appl. Microbiol. Biot. 80, 1-14.

Fisher R.G., Woods N.E., Fuchs H.E., Sweet R.M., 1980. Three-dimensional structures of C-Phycocyanin and B-Phycoerythrin at 5-A resolution, J. Biol. Chem. 255, 5082-5089.

Fleming B., Crerar D., 1982. Silicic acid ionization and calculation of silica solubility at elevated temperature and pH application to geothermal fluid processing and reinjection, Geothermics 11, 15-29.

Gallup D.L., Sugiaman F., Capuno V., Manceau A., 2003. Laboratory investigation of silica removal from geothermal brines to control silica scaling and produce usable silicates, Appl. Geochemi. 18, 1597-1612.

Grether-Beck S., Muhlberg K., Brenden H., Felsner I., Brynjolfsdottir A., Einarssson S., Krutmann J., 2008. Bioactive molecules from the Blue Lagoon: in vitro and in vivo assessment of silica mud and microalgae extracts for their effects on skin barrier function and prevention of skin ageing, Exp. Dermatol. 17, 771-779.

Hoffmann F., Cornelius M., Morell J., Froeba M., 2006. Silica-based mesoporous organic-inorganic hybrid materials, Angew. Chem. Int. Edition 45, 3216-3251.

Icopini G.A., Brantley S.L., Heaney P.J., 2005. Kinetics of silica oligomerization and nanocolloid formation as a function of pH and ionic strength at 25 degrees C, Geochim. Cosmochim. AC. 69, 293-303.

Jespersen L., Stromdahl L.D., Olsen K., Skibsted L.H., 2005. Heat and light stability of three natural blue colorants for use in confectionery and beverages, Eur. Food Res. Technol. 220, 261-266.

Johnston J.H., McFarlane A.J., Borrmann T., Moraes J., 2004. Nano-structured silica and silicates – new materials and their applications in paper, Curr. Appl. Phys. 4, 411-414.

McCall R., 1998. Cyanobacterial phycobilisomes, J. Struct. Biol. 124, 311-334.

McKeown A., Euerby M., Lomax H., Johnson C., Richie H., Woodruff M., 2001. The use of silica for liquid chromatographic/mass spectrometric, J. Sep. Sci. 24, 835-842.

Mishra S.K., Shrivastav A., Mishra S., 2008. Effect of preservatives for food grade C-PC from spirulina platensis, Process Biochem. 43, 339-345.

Patil G., Chethana S., Sridevi A., Raghavarao K., 2006. Method to obtain C-Phycocyanin of high purity, J. Chromatogr. A 1127, 76-81.

Paul-Dauphin S., Karaca F., Morgan T.J., Millan-Agorio M., Herod A.A., Kandiyoti R., 2007. Probing size exclusion mechanisms of complex hydrocarbon mixtures: The effect of altering eluent compositions, Energ. Fuel 21, 3484-3489.

Petursdottir S.K., Bjornsdottir S.H., Hreggvidsson G.O., Hjorleifsdottir S., Kristjansson J.K., 2009. Analysis of the unique geothermal microbial ecosystem of the Blue Lagoon, FEMS Microbiol. Ecol. 70, 425-432.

Petursdottir S.K., Kristjansson J.K., 1997. Silicibacter lacuscaerulensis gen. nov., sp. nov., a mesophilic moderately halophilic bacterium characteristic of the Blue Lagoon geothermal lake in Iceland, Extremophiles 1, 94-99.

Ramos A., Gabriel Acien F., Fernandez-Seville J.M., Gonzalez C.V., Bermejo R., 2010. Large-scale isolation and purification of C-phycocyanin from the cyanobacteria Anabaena marina using expanded bed adsorption chromatography, J. Chem. Technol. Biot. 85, 783-792.

Rito-Palomares M., Nunez L., Amador D., 2001. Practical application of aqueous two-phase systems for the development of a prototype process for C-Phycocyanin recovery from spirulina maxima, J. Chem. Technol. Biot. 76, 1273-1280.

Saemundsson K., Johannesson H., Hjartarson A., Kristinsson S.G., Sigurgeirsson M.A., 2010. Geological map of southwest Iceland, Iceland GeoSurvey, scale 1:100.000.

Tarasevich Y.I., Nazarenko A.V., Bondarenko S.V., 1990. Preparation, properties and chromatographic applications of natural and synthetic amorphous silica modified by organosilicate substances, Abstr. Pap. Am. Chem. S. 200, 186.

Zhang A., Xiao C., Xue W., Chai Z., 2009. Chromatographic separation of cesium by a macroporous silica-based supramolecular recognition agent impregnated material, Sep. Purif. Technol. 66, 541-548.

Figure captions:

Fig. 1. A flow sheet of the C-PC extraction process.

Fig. 2. Separation of C-PC at different stages in chronological order: (a) at early stage of the loading, (b) after loading with 190 ml crude extract, (c) after flushing with 2.2 l of brine solution (25% BL-salt in deionized water), and (d) after elution with 2.0 l deionized water.

Fig. 3. Concentration of C-PC (dashed line) and C-PC purity (solid line) as a function of eluent volume.

Fig. 4. Absorption spectra for algae extracts of different purity: crude extract (dotted line), collection #1 (dashed line), and collection #2 (solid line).

Fig. 5. X-ray diffraction pattern of BL-silica before (black solid line) and after sintering at 1000°C for 2 hours (red dotted line).

Fig. 6. SEM images at two different magnifications of the BL-silica: a) before sintering; and b) after sintering. The inset in b) shows crystals formed during the sintering process.

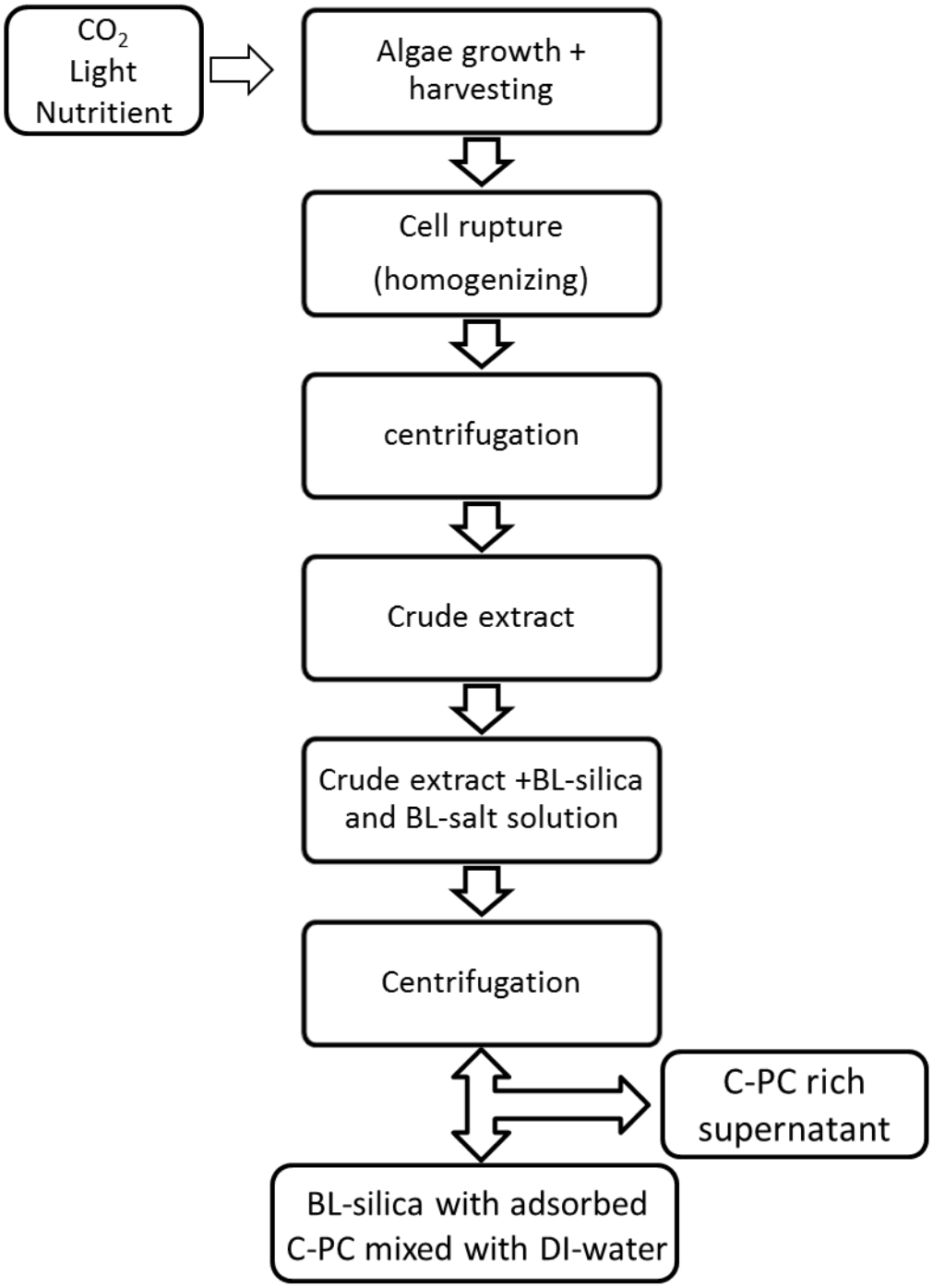
CO_2
Light
Nutritient
Algae growth + harvesting
Cell rupture (homogenizing)
centrifugation
Crude extract
Crude extract +BL-silica and BL-salt solution
Centrifugation
C-PC rich supernatant
BL-silica with adsorbed C-PC mixed with DI-water

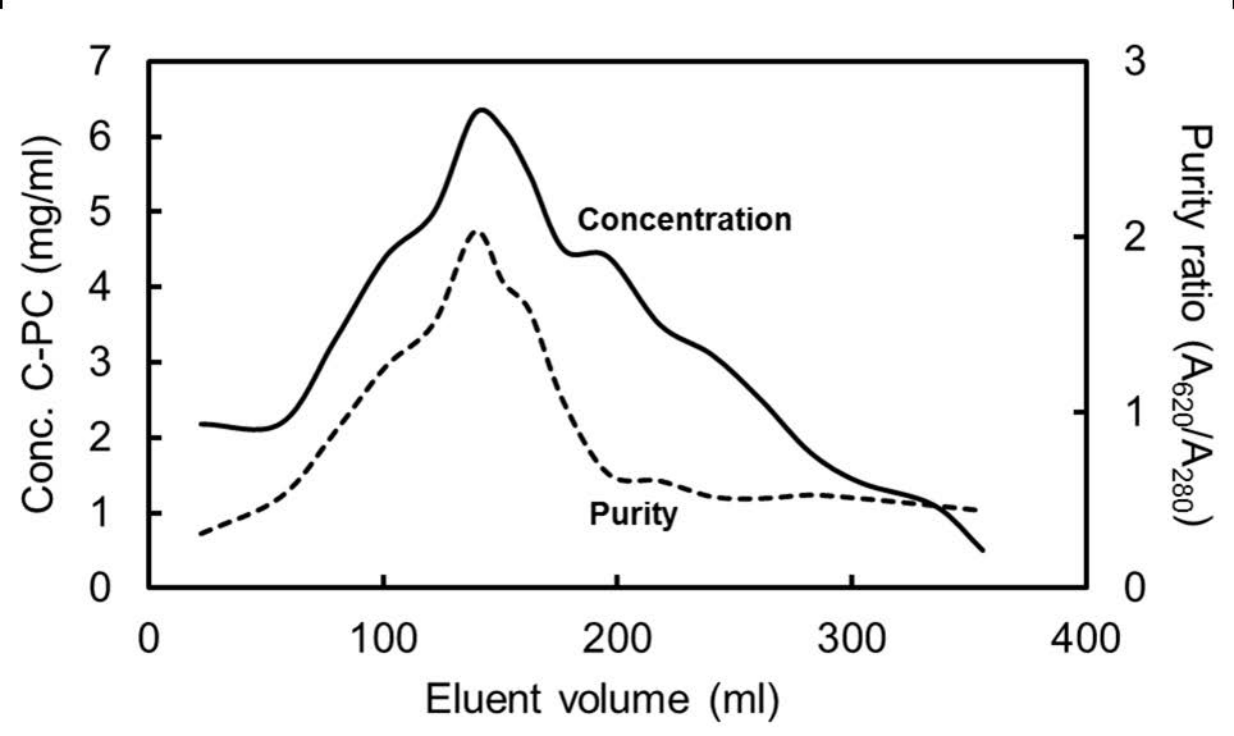
Conc. C-PC (mg/ml)
Purity ratio (A_{620}/A_{280})
Concentration
Purity
Eluent volume (ml)
0
1
2
3
4
5
6
7
100
200
300
400

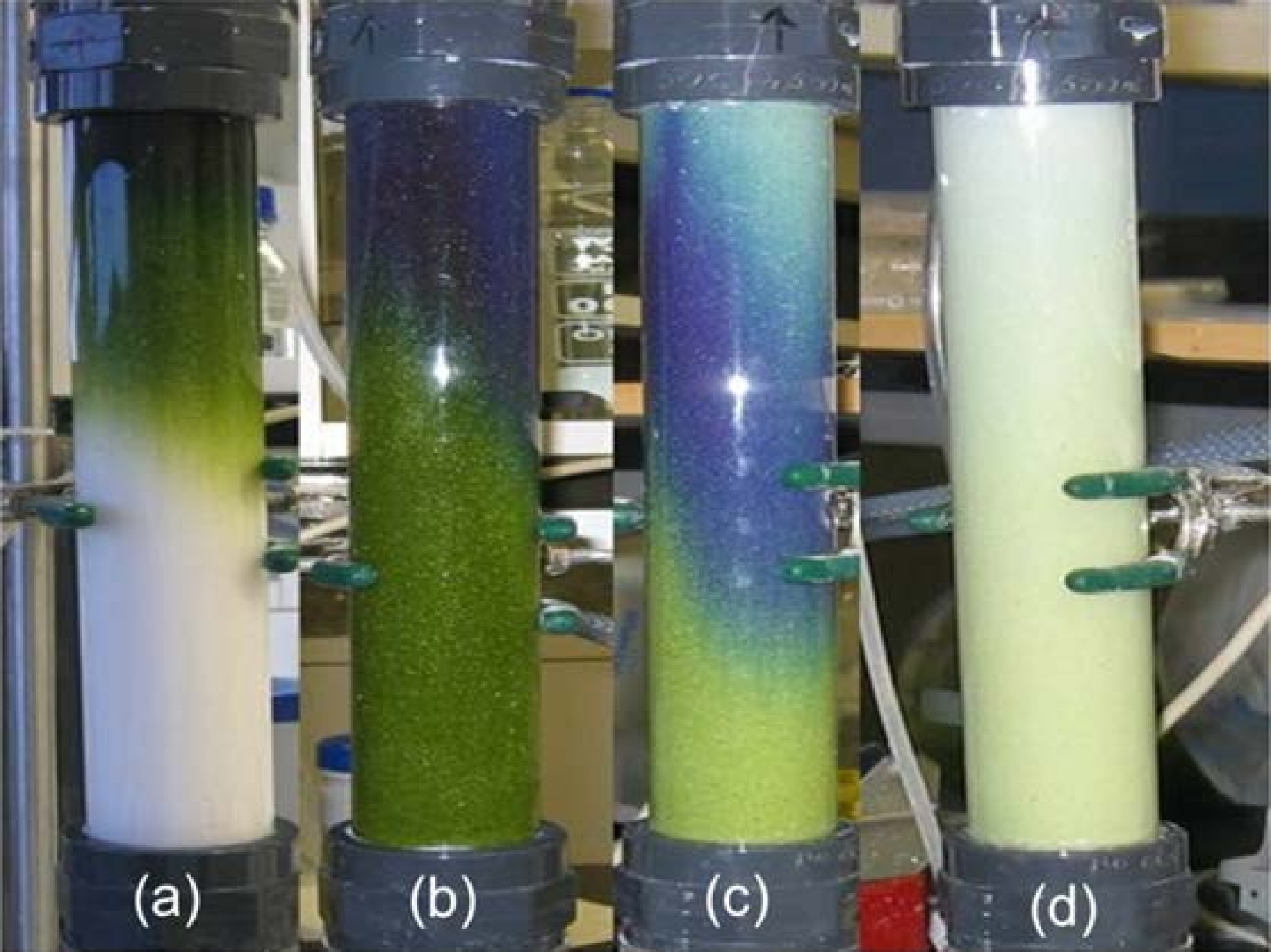
(a)
(b)
(c)
(d)

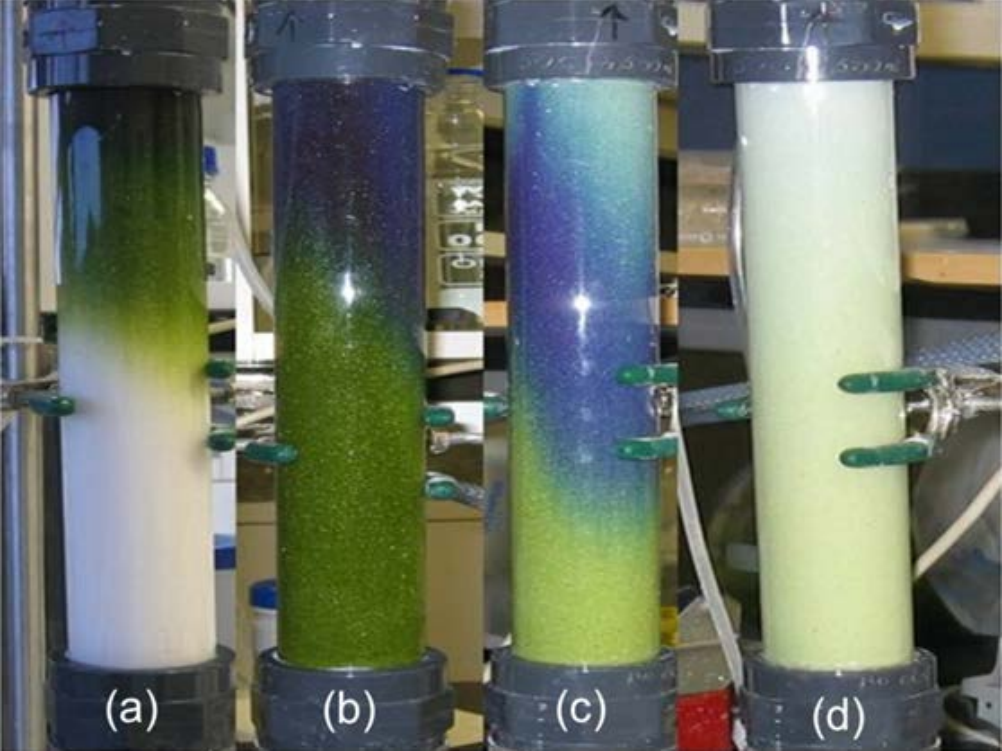
(a)
(b)
(c)
(d)

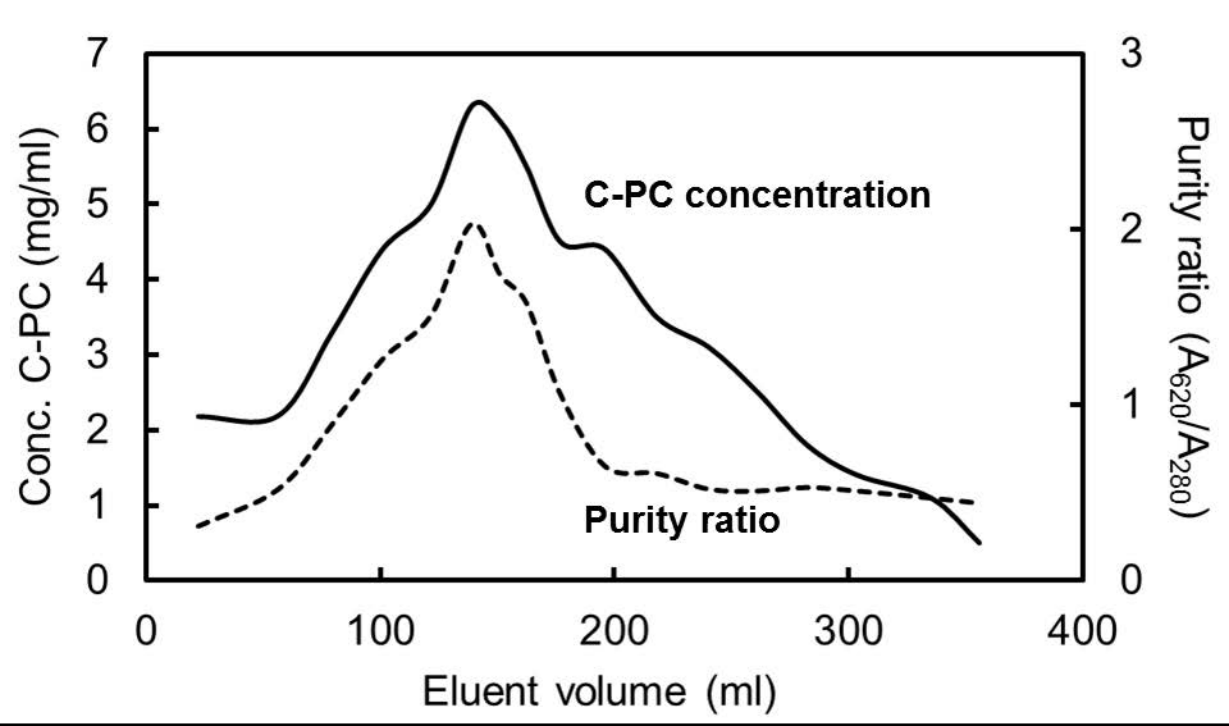
C-PC concentration
Purity ratio
Conc. C-PC (mg/ml)
Purity ratio (A_{620}/A_{280})
Eluent volume (ml)
0
1
2
3
4
5
6
7
0
100
200
300
400

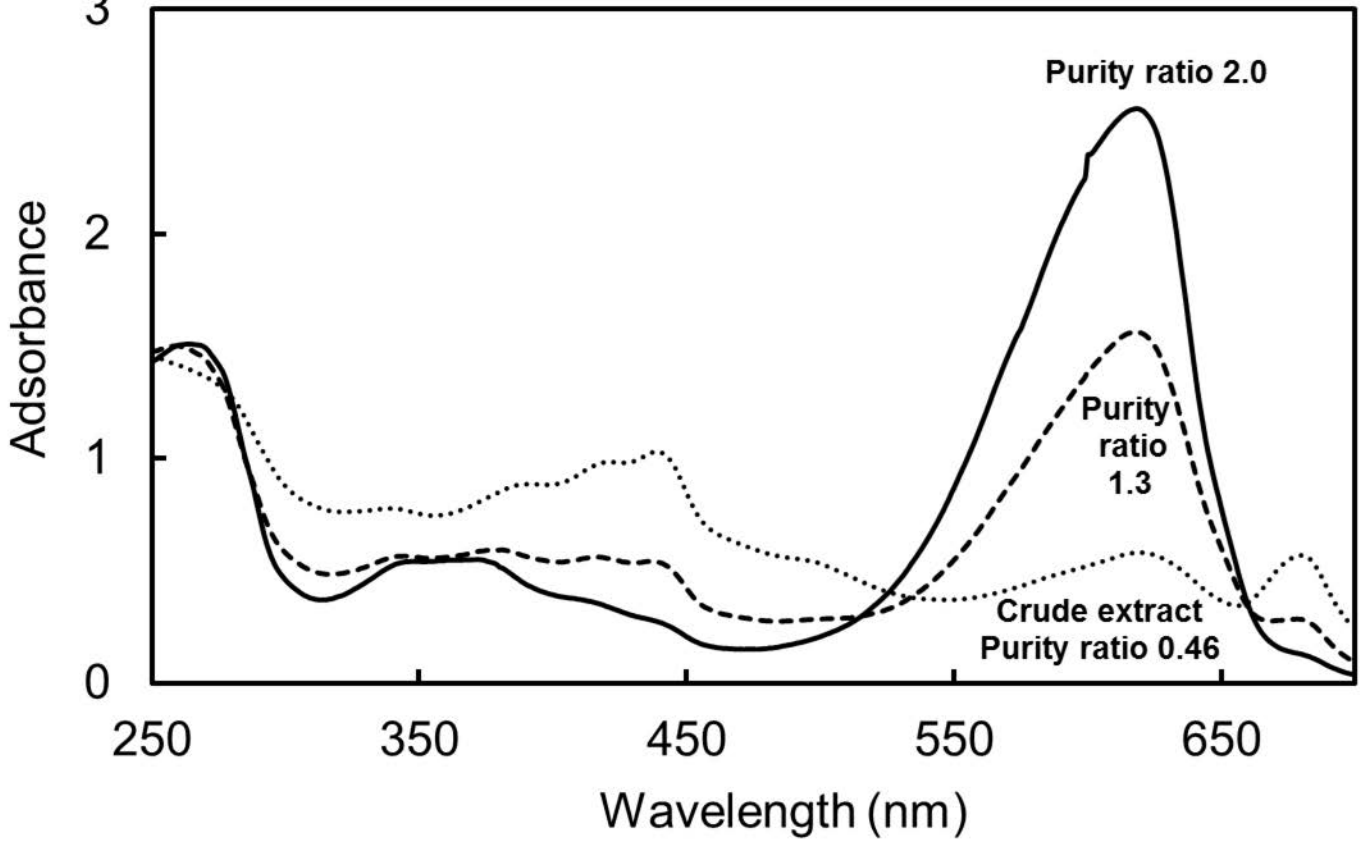
3
2
1
0
Adsorbance
250
350
450
550
650
Wavelength (nm)
Purity ratio 2.0
Purity
ratio
1.3
Crude extract
Purity ratio 0.46

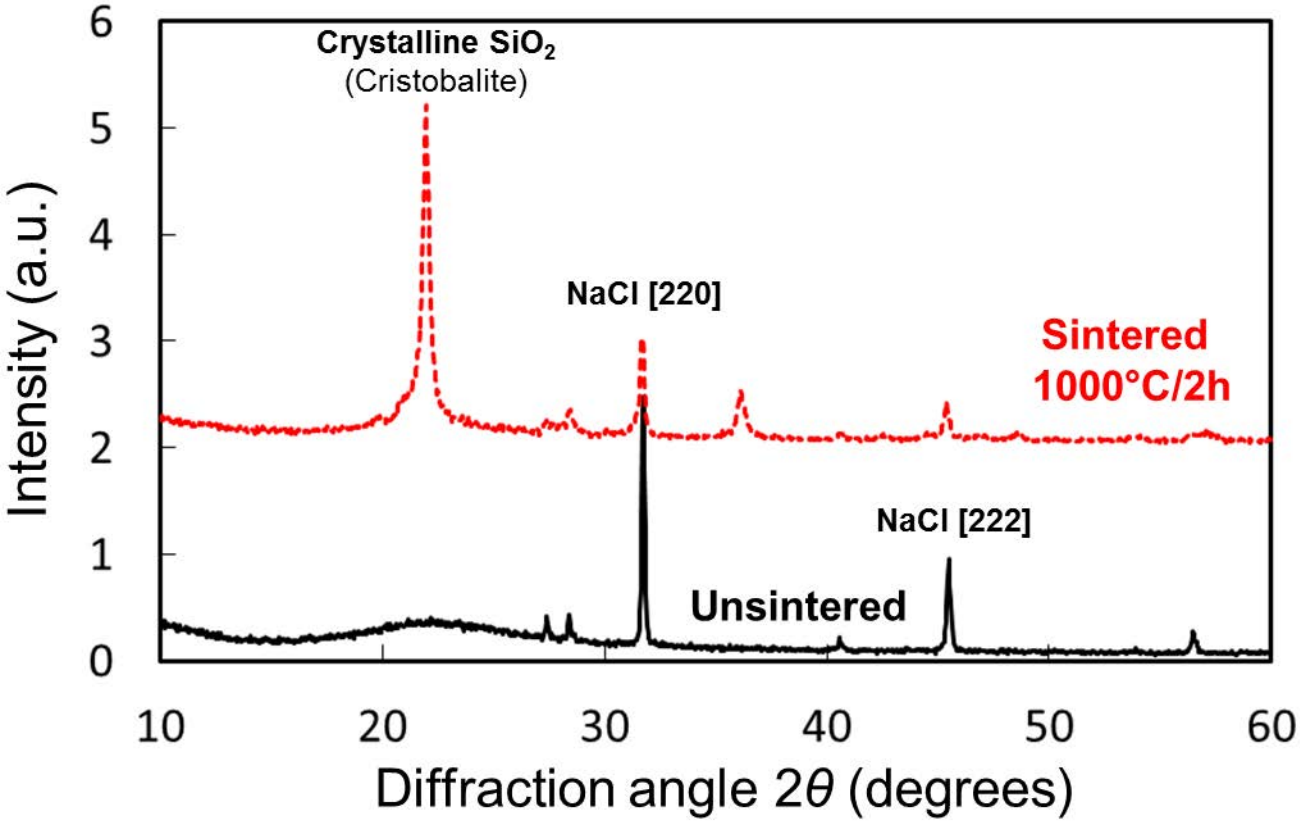
Crystalline SiO2
(Cristobalite)
NaCl [220]
Sintered
1000°C/2h
NaCl [222]
Unsintered
Intensity (a.u.)
Diffraction angle 2θ (degrees)
0
1
2
3
4
5
6
10
20
30
40
50
60

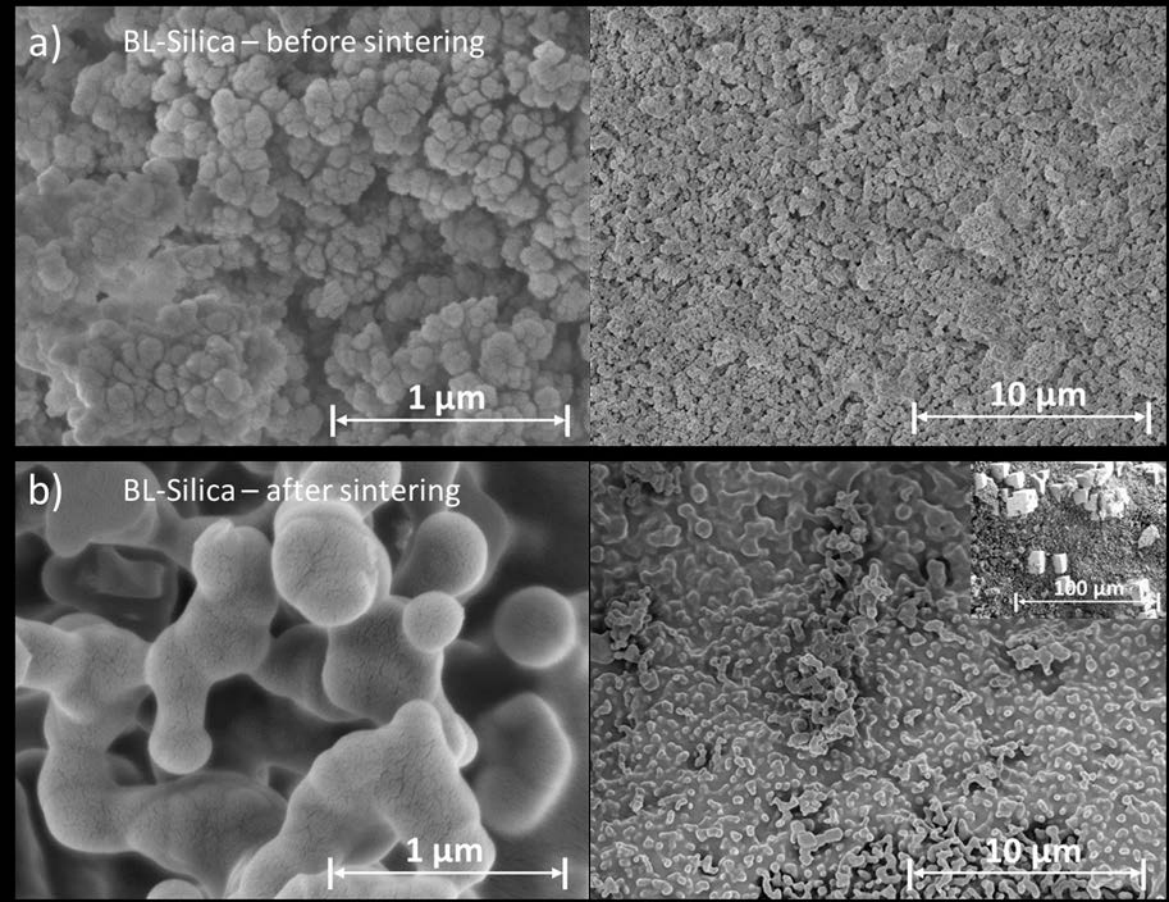
a)
BL-Silica – before sintering
1 µm
10 µm
b)
BL-Silica – after sintering
1 µm
100 µm
10 µm

Table 1. Surface characteristics of the BL-silica.

BL-silica	BET spec. surf. area [m^2/g]	Micropore surf. area t-Plot [m^2/g]	Vol. of pores with diameter 1.7 – 300 nm [cm^3/g]	BJH adsorption av. pore width [nm]
Unsintered	50	6	0.24	23
Sintered	1	0.3	0.001	N/A

Table 2. Chemical composition of BL-silica and BL-salt (wt. %).

Component	SiO_2	Cl	Na	Ca	K	Mg	Total
BL-silica	92.9	3.9	2.2	0.49	0.39	< 0.1	99.9
BL-salt	0.02	58.7	34.0	1.83	1.75	< 0.1	96.3